

Sub-Doppler Measurements of the Rotational Spectrum of $^{13}\text{C}^{16}\text{O}$

G. Klapper,* F. Lewen,* R. Gendriesch,* S. P. Belov,† and G. Winnewisser*

*I. Physikalisches Institut, Universität zu Köln, Zùlpicher Str. 77, D-50937 Cologne, Germany; and

†Institute of Applied Physics, Nizhnii Novgorod, 603 600, Russia

Received October 29, 1999; in revised form January 14, 2000

The five lowest J rotational transitions of $^{13}\text{C}^{16}\text{O}$ have been measured by saturation-dip spectroscopy to an accuracy of about 2 kHz, employing phase-stabilized backward-wave oscillators (BWOs). These highly precise measurements cover the transitions from $J = 2 \leftarrow 1$ to $J = 6 \leftarrow 5$ with frequencies ranging from 220 to 661 GHz. For each of the five observed rotational transitions, the narrow linewidths of the saturation dips (about 20 kHz) permitted the resolution of the hyperfine splitting for the first time. This splitting is caused by the ^{13}C -nuclear spin-rotation interaction yielding a value for the nuclear spin-rotation coupling constant of $C_I(^{13}\text{C}^{16}\text{O})$. If combined with the beam measurements ($C_I(^{13}\text{C}^{16}\text{O}) = 32.63(10)$ kHz), a slight J -dependence of the spin-rotation coupling constant can be determined ($C_J = 30 \pm 13$ Hz). In addition, we have measured in the Doppler-limited mode several higher J rotational line positions of $^{13}\text{C}^{16}\text{O}$ up to 991 GHz with an accuracy of 5 kHz. The two line positions ($J = 12 \leftarrow 11$ and $J = 14 \leftarrow 13$) were recorded by multiplying BWO frequency with an accuracy of 100 kHz. The rotational transitions $J = 17 \leftarrow 16$ and $J = 18 \leftarrow 17$ were measured with an accuracy between 15 and 25 kHz by using the Cologne sideband spectrometer for terahertz applications COSSTA. © 2000 Academic Press

INTRODUCTION

Precisely measured rest frequencies of the rotational transitions of several selected molecules with relatively simple, but uncongested line patterns serve in the laboratory as easy but rather important secondary frequency calibration standards. The pure rotational spectrum of CO is ideally suited for this purpose and the spectrum of the main isotopomer, $^{12}\text{C}^{16}\text{O}$, has for a long time been used as a secondary standard. Consequently, the quality of the rest frequency determination of line positions has always reflected the state of the art in terms of accuracy (1, 2). Despite the importance and the need of precisely known rest frequencies for CO transitions, for laboratory and astrophysical requirements alike, the work on the precise determination of additional rest frequencies concerning the rarer isotopomers of CO has remained remarkably incomplete and patchy up until the early 1990s. Aside from the sub-Doppler measurements on the main isotopomer $^{12}\text{C}^{16}\text{O}$ by Winnewisser *et al.* (3) and the Doppler-limited sideband measurements of the far-infrared rotational transitions by Varberg and Evenson (2) for none of the other isotopomers, a similar range of highly precise (sub-Doppler) measurements exists. Zink *et al.* (4) reported the rotational spectrum of $^{13}\text{C}^{16}\text{O}$ measured with a tunable far-IR spectrometer in the frequency range between 0.6 and 3.3 THz.

So far the most complete microwave measurements carried out on six different CO isotopomers up to 576 GHz ($J = 5 \leftarrow 4$) were published by Winnewisser *et al.* (1). For these Doppler-limited measurements estimated accuracies on the line center determination ranged between 1 and 470 kHz, depending on the signal-to-noise ratio and the blending of the lines

due to unresolved hyperfine structure. However, for the rarer isotopomers of CO these measurements were limited to the frequency range below about 500 GHz. With the technical capability at hand to perform highly precise measurements up to 2 THz, we decided to carry out the task of measuring the rotational spectra of the various CO isotopomers.

EXPERIMENTAL DETAILS

Two spectrometers were used for the measurements, the Cologne terahertz spectrometer (5) and the Cologne sideband spectrometer for terahertz applications (6). Both spectrometers operate with phase-locked BWOs and in the case of the sideband spectrometer with a frequency-locked FIR laser. All reference frequencies are locked against a rubidium frequency standard. The Cologne terahertz spectrometer can be used up to about 1 THz in the sub-Doppler mode. In addition, beyond 1.3 THz frequency multiplication of the BWO was applied here. The present measurements on $^{13}\text{C}^{16}\text{O}$ have been carried out with both spectrometers, and five transitions (<700 GHz) have been measured with sub-Doppler resolution. In this case the integration time for each data point was about 3.1 s. The total scan consists of 160 data points.

RESULTS

In Table 1 the frequencies of the newly measured transitions of $^{13}\text{C}^{16}\text{O}$ are summarized together with the transition frequency of the $J = 1 \leftarrow 0$ line measured by Winnewisser *et al.* (1) and the measurements by Zink *et al.* (4). The line center frequencies were derived from the measured data points by fitting them to a para-

TABLE 1
Sub-Doppler and Doppler-Resolved Rotational
Transitions of $^{13}\text{C}^{16}\text{O}$

J'	F'	\leftarrow	J''	F''	Obs. Frequencies ^a [MHz]	O-C [kHz]	Rel. Int.
1		\leftarrow	0		110 201.3541(51) ^b	0.2	
2	1.5	\leftarrow	1	1.5	220 398.619(10) ^c	5.2	0.067
2	1.5	\leftarrow	1	0.5	220 398.6635(20) ^c	-2.5	0.333
2	2.5	\leftarrow	1	1.5	220 398.6998(20) ^c	-1.1	0.600
3	2.5	\leftarrow	2	1.5	330 587.9470(20) ^c	0.1	0.400
3	3.5	\leftarrow	2	2.5	330 587.9802(20) ^c	-1.5	0.571
4	3.5	\leftarrow	3	2.5	440 765.1556(20) ^c	0.1	0.429
4	4.5	\leftarrow	3	3.5	440 765.1903(20) ^c	0.6	0.556
5	4.5	\leftarrow	4	3.5	550 926.2663(20) ^c	-0.1	0.444
5	5.5	\leftarrow	4	4.5	550 926.3016(20) ^c	0.4	0.546
6	5.5	\leftarrow	5	4.5	661 067.2586(20) ^c	0.6	0.455
6	6.5	\leftarrow	5	5.5	661 067.2936(20) ^c	0.8	0.539
7		\leftarrow	6		771 184.125(5) ^c	0.6	
8		\leftarrow	7		881 272.808(5) ^c	-0.6	
9		\leftarrow	8		991 329.305(5) ^c	-1.6	
11		\leftarrow	10		1 211 329.636(50) ^d	-26.9	
12		\leftarrow	11		1 321 265.42(10) ^e	-63.2	
14		\leftarrow	13		1 540 988.23(10) ^e	-91.5	
15		\leftarrow	14		1 650 767.344(55) ^d	35.0	
17		\leftarrow	16		1 870 140.359(25) ^f	3.7	
18		\leftarrow	17		1 979 726.393(15) ^f	0.2	
19		\leftarrow	18		2 089 240.033(55) ^d	-62.4	
25		\leftarrow	24		2 744 579.059(60) ^d	-32.4	
26		\leftarrow	25		2 853 474.444(60) ^d	40.1	
28		\leftarrow	27		3 070 948.140(70) ^d	56.2	
30		\leftarrow	29		3 287 972.525(100) ^d	-82.4	

^a For unresolved hyperfine structure the F values and relative intensities are omitted. In these cases the calculated frequencies were obtained by using intensity weighted averages of individual hfs components. See text.

^b Observed frequency taken from Winnemisser *et al.* (1).

^c Frequencies measured with the Cologne terahertz spectrometer.

^d Frequencies taken from Zink *et al.* (4).

^e Frequencies were recorded by multiplying the BWO output.

^f Frequencies measured with the Cologne sideband spectrometer.

bolic function. Although the achieved measurement accuracies depend on the spectrometer used and on the mode of operation employed, the Cologne Doppler-limited measurements (<1 THz) can be trusted to 5 kHz, whereas the present Lamb-dip measurements should be reliable to about 2 kHz. It should be noted that the quoted uncertainties for the Lamb-dip measurements represent in this case not the ultimately reachable measurement accuracy of the spectrometer, but rather reflect the fact that the two strongest hyperfine components are slightly overlapping. Extracting under these conditions the optimal information from the experimental data set is very much a data-handling problem and will be discussed elsewhere (7).

However, here the apparatus function is represented by the monochromaticity of the BWO signal. Ultrahigh-resolution spectra of the down-converted BWO signal at the phase-lock loop intermediate frequency (IF) have been performed, and the measured half-power linewidth was less than 0.1 Hz (8). It is

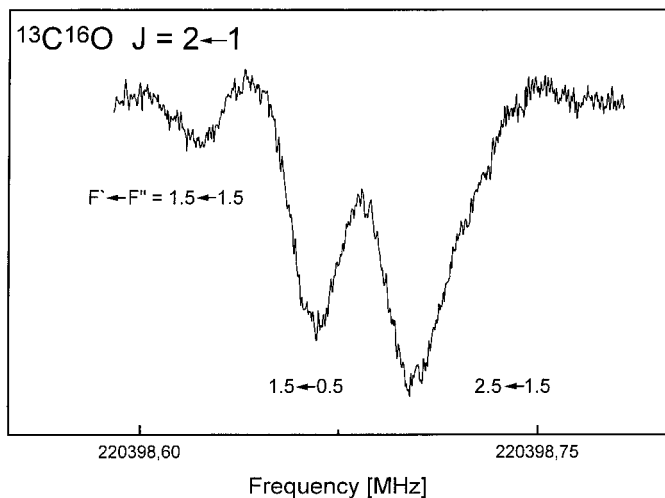


FIG. 1. The Lamb-dip spectrum of the $J = 2 \leftarrow 1$ transition of $^{13}\text{C}^{16}\text{O}$ at 220 GHz.

expected that an apparatus function as narrow as this will have a negligible effect on the observed line profile. A more severe influence on the linewidth is caused by the modulation broadening, which can be seen as a trade-off between line broadening and the signal-to-noise ratio of the spectra. We kept the influence to a level below 15 kHz by choosing a low-modulation frequency (7.3 kHz) and an appropriate frequency-modulation width (approximately 80% of the linewidth). Furthermore, since time-of-flight, as well as power broadening, and pressure effects are evident, the optimum parameters for a minimum linewidth have been experimentally determined for

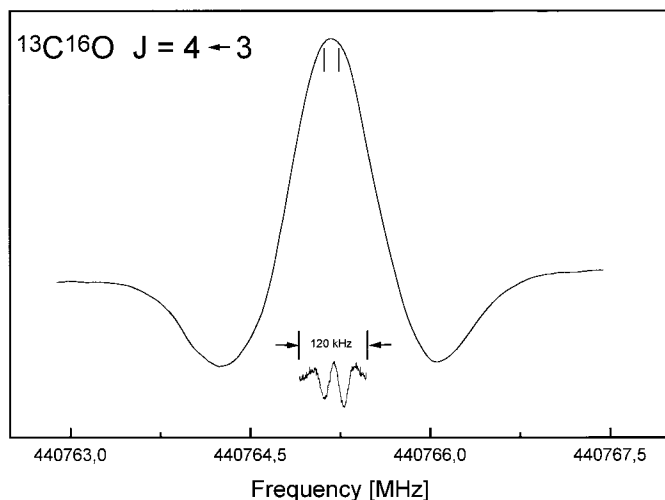


FIG. 2. The Doppler and the sub-Doppler spectrum of the $J = 4 \leftarrow 3$ transition of $^{13}\text{C}^{16}\text{O}$ at 440 GHz. The scanwidth is 4.6 MHz in the Doppler mode and 120 kHz in the sub-Doppler mode. For the sub-Doppler spectrum the frequency scale is magnified by a factor about 5. The two markers at the Doppler spectrum indicate the corresponding begin and end of the Lamb-dip spectrum. The width of the Doppler line is about 760 kHz and that of each sub-Doppler line 18 kHz.

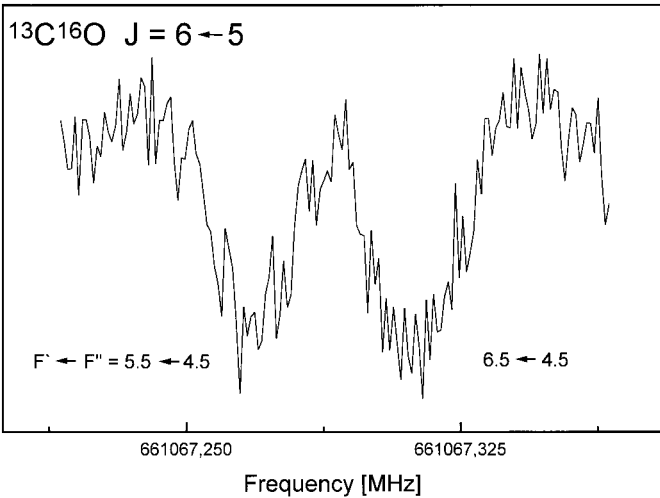


FIG. 3. The highest J rotational transition of $^{13}\text{C}^{16}\text{O}$ measured in sub-Doppler resolution at 661 GHz.

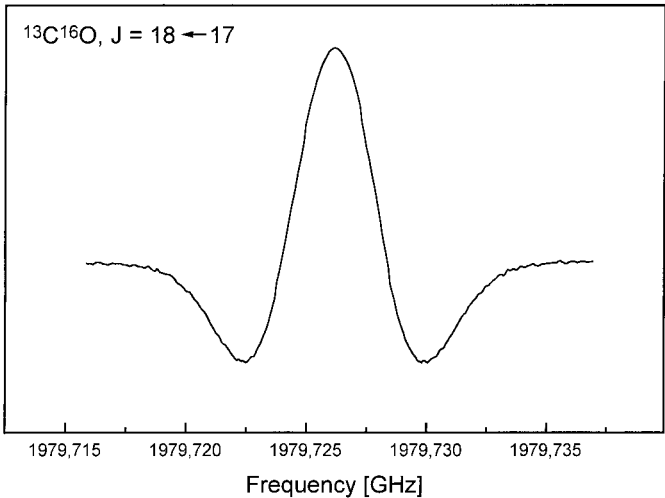


FIG. 4. The Doppler spectrum of the $J = 18 \leftarrow 17$ transition, measured with the Cologne sideband spectrometer for THz applications (COSSTA).

each line. Other experimental effects, like optical misalignment, or baseline problems have been minimized for each line position, separately. However, the achievable accuracy for unblended, fully resolved Lamb-dip measurements in the sub-millimeter-wave region recorded with a good signal-to-noise ratio is estimated to be around 500 Hz (3).

In a series of figures we present some of the recorded Lamb-dip spectra. Figure 1 displays a recording of the central portion of the $J = 2 \leftarrow 1$ transition. For these transitions the splitting is due to the ^{13}C -nuclear spin-rotation hyperfine structure. This triplet hyperfine structure observed for the $J = 2 \leftarrow 1$ transition is superimposed on its Doppler profile. The total width of this triplet is about 80 kHz, and the two strongest components are separated by only 36.3 kHz. The weakest of the three hyperfine components $F' \leftarrow F'' = 1.5 \leftarrow 1.5$ could be secured after subtraction of a second-order baseline. The full linewidths of the hyperfine components range between 18

and 25 kHz, just allowing the resolution of the two main hyperfine components. With the exception of the weakest component, to which we assign an accuracy of ± 10 kHz, the center frequencies of the two stronger hyperfine components are measured to better than 2 kHz, or to about one part in 10^9 .

Figure 2 presents a composite of the Doppler and sub-Doppler profile of the $J = 4 \leftarrow 3$ transition at 440 GHz. The width of the Doppler profile is close to 760 kHz, whereas the linewidths of the two hyperfine components are about 18 kHz each, with a separation of 34.8 kHz. In Fig. 3 we present the highest frequency Lamb-dip spectrum recorded in this study, the two strongest hyperfine components of the $J = 6 \leftarrow 5$ rotational transition. A recording of the $J = 18 \leftarrow 17$ transition at 1.979 THz is shown in Fig. 4.

The new set of data of $^{13}\text{C}^{16}\text{O}$ was subjected to a least-square fit in which each line was weighted proportionally to the inverse square of its assigned experimental uncertainty. For unresolved

TABLE 2
Molecular Constants of $^{13}\text{C}^{16}\text{O}$

Constant	This work	MMW data ^a	IR data ^b	Molecular beam	Unit
B_0	55101.009476(43)	55101.009484(45)	55101.0098(9)	55101.0125(22)	— MHz
D_0	167.68467(61)	167.68470(65)	167.602(23)	167.6611(27)	— kHz
H_0	0.14956(63)	0.14958(66)	0.1435 ^c	0.14353(66)	— Hz
C_I	34.82(35)	32.63(10) ^d	—	—	32.57(22) ^e kHz
					32.70(12) ^f kHz
C_J	—	30(13)	—	—	— Hz

^a Winnewisser *et al.* (1).
^b Values derived from Guelachvili *et al.* (9).
^c Fixed from Ref. (9).
^d Fixed to the average from Ozier *et al.* (10) and Meerts *et al.* (11).
^e Ozier *et al.* (10). The value has been averaged and converted to the present sign convention.
^f Meerts *et al.* (11).

TABLE 3
Predicted Frequencies of $^{13}\text{C}^{16}\text{O}$
Rotational Transitions

J'	$\leftarrow J''$	Cal. Frequencies ^a [MHz]
1	$\leftarrow 0$	110 201.35393(12)
2	$\leftarrow 1$	220 398.68346(23)
3	$\leftarrow 2$	330 587.96427(32)
4	$\leftarrow 3$	440 765.17231(39)
5	$\leftarrow 4$	550 926.28381(44)
6	$\leftarrow 5$	661 067.27544(51)
7	$\leftarrow 6$	771 184.12442(65)
8	$\leftarrow 7$	881 272.80861(90)
9	$\leftarrow 8$	991 329.3066(13)
10	$\leftarrow 9$	1 101 349.5979(18)
11	$\leftarrow 10$	1 211 329.6629(25)
12	$\leftarrow 11$	1 321 265.4832(34)
13	$\leftarrow 12$	1 431 153.0414(44)
14	$\leftarrow 13$	1 540 988.3215(57)
15	$\leftarrow 14$	1 650 767.3090(71)
16	$\leftarrow 15$	1 760 485.9908(88)
17	$\leftarrow 16$	1 870 140.355(11)
18	$\leftarrow 17$	1 979 726.393(13)
19	$\leftarrow 18$	2 089 240.095(15)
20	$\leftarrow 19$	2 198 677.457(18)
21	$\leftarrow 20$	2 308 034.474(21)
22	$\leftarrow 21$	2 417 307.144(24)
23	$\leftarrow 22$	2 526 491.468(28)
24	$\leftarrow 23$	2 635 583.449(32)
25	$\leftarrow 24$	2 744 579.091(36)
26	$\leftarrow 25$	2 853 474.404(41)
27	$\leftarrow 26$	2 962 265.397(46)
28	$\leftarrow 27$	3 070 948.084(52)
29	$\leftarrow 28$	3 179 518.481(58)
30	$\leftarrow 29$	3 287 972.607(64)
31	$\leftarrow 30$	3 396 306.486(71)
32	$\leftarrow 31$	3 504 516.142(78)
33	$\leftarrow 32$	3 612 597.605(86)
34	$\leftarrow 33$	3 720 546.906(94)
35	$\leftarrow 34$	3 828 360.08(10)
36	$\leftarrow 35$	3 936 033.18(11)
37	$\leftarrow 36$	4 043 562.22(12)
38	$\leftarrow 37$	4 150 943.28(13)
39	$\leftarrow 38$	4 258 172.39(14)
40	$\leftarrow 39$	4 365 245.62(15)

^a For frequencies the hfs and relative intensity is omitted.

hyperfine splittings, the calculated frequencies were determined in the fit by using intensity-weighted averages of the individual hyperfine components. In Table 2 we give a summary of the newly determined three rotational constants B_0 , D_0 , and H_0 together with the nuclear spin-rotation constant $C_I(^{13}\text{C}^{16}\text{O})$. The values of the three rotational constants generally agree with the appropriate values quoted by Winnemisser *et al.* (1) and Guelachvili *et al.* (9). The constants fitted by Guelachvili *et al.* (9) are based on a large set of IR data ranging from 1205 to 6335 cm^{-1} .

The new set of constants reproduces the experimental data very well as can be seen by the $o - c$ values given in Table 1. The value of $C_I = 34.82 \pm 0.35$ kHz (Table 2 first column) can be compared with the one reported by Ozier *et al.* (10) ($C_I = 32.57 \pm 0.22$ kHz). This value has been averaged and converted to present sign convention. Meerts *et al.* (11) give $C_I = 32.70 \pm 0.12$ kHz. They obtained C_I from molecular beam magnetic-resonance experiments.

In checking whether our measurements could reveal a J -dependence of C_I , two different tests were performed: first, we determined C_I from our sub-Doppler data with a result in Table 2 (first column). In addition to C_I we tried to include C_J as a free variable in our fitting procedure. $C_J = 3 \pm 23$ Hz cannot be determined uniquely. In a second attempt, we fixed $C_I = 32.63 \pm 0.10$ kHz to the average value of Ozier *et al.* (10) and Meerts *et al.* (11) and fitted C_J as a variable resulting in a value of 30 ± 13 Hz. However, we feel that the determination of this value is at the limit of our sub-Doppler measurements.

Table 3 gives a listing of the predicted $^{13}\text{C}^{16}\text{O}$ -rotational transition frequencies up to the $J = 40 \leftarrow 39$ transition, which are thought to be of use to future astronomical searches with the SOFIA facility, for example. The uncertainties of the predicted frequencies are based only on the accuracies of the constants used. Higher order parameters not determined here are neglected. The higher order term L_0 seems to be of no significance (3). We have performed similar measurements on other isotopomers of CO and these data sets are presently being prepared for publication.

ACKNOWLEDGMENTS

We thank the unknown referee for his constructive comments on the J -dependence of the spin-rotation constant. This work was supported in part by the Deutsche Forschungsgemeinschaft (DFG) via Grant SFB 301 and special funding from the Science Ministry of the State Nordrhein-Westfalen. The work of S.P.B. at Cologne was made possible by the DFG through grants aimed to support Eastern and Central European Countries and the republics of the former Soviet Union, which is gratefully acknowledged.

REFERENCES

1. M. Winnemisser, B. P. Winnemisser, and G. Winnemisser, in "Molecular Astrophysics, Series C," Vol. 157, pp. 375–402, Reidel, Dordrecht, 1985.
2. T. D. Varberg and K. M. Evenson, *Astrophys. J.* **385**, 763–765 (1992).
3. G. Winnemisser, S. P. Belov, Th. Klaus, and R. Schieder, *J. Mol. Spectrosc.* **184**, 468–472 (1997).
4. L. R. Zink, P. De Natale, F. S. Pavone, M. Prevedelli, K. M. Evenson, and M. Inguscio, *J. Mol. Spectrosc.* **143**, 304–310 (1990).
5. G. Winnemisser, *Vib. Spectrosc.* **8**, 241–253 (1995).
6. F. Lewen, E. Michael, R. Gendriesch, J. Stutzki, and G. Winnemisser, *J. Mol. Spectrosc.* **183**, 207–209 (1997).
7. Š. Urban, G. Winnemisser, and K. M. T. Yamada, submitted for publication.
8. F. Lewen, R. Gendriesch, I. Pak, D. G. Paveliev, M. Hepp, R. Schieder, and G. Winnemisser, *Rev. Sci. Instrum.* **69**, 32–39 (1998).
9. G. Guelachvili, G. De Villeneuve, R. Farrenq, W. Urban, and J. Verges, *J. Mol. Spectrosc.* **98**, 64–79 (1983).
10. I. Ozier, L. M. Crapo, and N. F. Ramsey, *J. Chem. Phys.* **49**, 2314–2321 (1968).
11. W. L. Meerts, F. H. de Leeuw, and A. Dymanus, *Chem. Phys.* **22**, 319–324 (1977).